Journal of Power Sources 183 (2008) 339–343

Contents lists available at ScienceDirect

Journal of Power Sources

journal homepage: www.elsevier.com/locate/jpowsour

Short communication

The role of the morphology in the response of Sb–C nanocomposite electrodes in lithium cells

Jusef Hassoun[a], Gaelle Derrien[b], Stefania Panero[a], Bruno Scrosati[a,*]

[a] Department of Chemistry, University of Rome "La Sapienza", Piazza Aldo Moro 5, 00185 Rome, Italy
[b] ICG-AIME CNRS UMR 5253, Université Montpellier II, CC 015, Place E. Bataillon, 34095 Montpellier Cedex 5, France

ARTICLE INFO

Article history:
Received 18 March 2008
Received in revised form 28 April 2008
Accepted 1 May 2008
Available online 14 May 2008

Keywords:
Antimony
Carbon
Nanocomposite
Anode
Lithium
Battery

ABSTRACT

This work reports an electrochemical study of antimony-carbon composites. The study has been carried out by testing in lithium cells two samples of Sb–C electrodes, differing by the relative composition and by the dimensions of the antimony particles. The results show that the particle size has crucial role in influencing the cycling response of the Li–Sb cells in terms of the extent and the maintenance of the capacity delivery.

1. Introduction

Extensive work is presently addressed to lithium batteries with the aim of upgrading their performance in order to make them as suitable power sources for electric or hybrid vehicles. Indeed, for meeting the vehicle requirements, lithium batteries still require improvements in terms of energy and power content. So far, the energy density of these batteries has been increased mostly by engineering optimization, e.g., by reducing the weight of the cases and/or by increasing the loading of the active materials, however, without changing the basic chemistry which still involves a graphite anode, an organic lithium conducting electrolyte and a layered lithium oxide, usually lithium cobalt oxide [1]. At the present stage a limit has been reached beyond which further improvements in energy density can only by obtained by switching to new high capacity electrode materials. In this respect, lithium metal alloys, such as lithium–silicon, Li–Si and lithium–tin, Li–Sn, are very attractive alternatives since their specific capacity largely exceeds that of commercial graphite, i.e. 4200 mAh g^{-1} and 993 mAh g^{-1} versus 370 mAh g^{-1} [2–4].

Consequently, much attention has been addressed to the study of these lithium alloys with the goal of optimizing their electrode performance. The results of these studies are impressive. The main issue which used to affect the response of the alloy electrodes in lithium batteries, i.e. the strain associated with the large volume changes which accompany their electrochemical process, has been circumvented by passing from bulk structures to nanostructures, such as reducing the particles size to nanodimensions [5,6] or by dispersing them in carbon matrices [7].

Not comparable attention has been devoted to alloys others than Li–Si and Li–Sn. This is surprising since there are interesting alternatives. One is the lithium–antimony, Li–Sb, alloy whose theoretical capacity, although lower than that of Li–Si or Li–Sn, is still at the remarkable level of 660 mA g^{-1}. There may be various reasons for this lack of interest, one possibly associated with the partially toxicity of antimony and the other, perhaps more relevant, to an expected poor electrode performance. Indeed, literature works generally suggest that the Li–Sb electrodes cannot be efficiently cycled in lithium cells, since their capacity remains at high values only for few cycles, to then abruptly decays [8–14].

It has appeared to us of interest to extend the investigation of the Li–Sb system mainly with the aim of establishing whether, as in the Li–Si and Li–Sn cases, also the Li–Sb electrochemical performance could be improved by switching to nanostructures and in particular, to the carbon composite nanostructures which had proven to the successful in stabilizing the behaviour of tin-based electrodes [7]. Two samples of Sb–C composites, differing by the composition and

* Corresponding author. Tel.: +39 06 4462866; fax: +39 06 491769.
E-mail address: bruno.scrosati@uniroma1.it (B. Scrosati).

0378-7753/$ – see front matter © 2008 Elsevier B.V. All rights reserved.
doi:10.1016/j.jpowsour.2008.05.017

by the size of the antimony particles within the carbon structure, have been prepared and characterized in lithium cells. The results are reported in this work.

2. Experimental

The Sb–C nanostructured composite was prepared following a synthesis pathway developed in the laboratory for preparation of Sn-C nanocomposite material [7]. Typically, a resorcinol-formaldehyde gel was prepared using 12 mmol resorcinol (Aldrich, 98%) and 24 mmol formaldehyde (Aldrich, 37 wt% in water, ACS reagent) mixed in 3 mL water, using potassium carbonate (K_2CO_3, Sigma, 99%+) as catalyst. After stirring at 70 °C, the gel was aged overnight, gently ground and finally washed with water. Next a solvent exchange was carried out from water to tertio-butanol (Aldrich, 99%+) and then the gel was immersed in a solution of triphenylantimony(III) (Aldrich, 99%) and toluene (Aldrich, puriss.)/tertio-butanol, in a mass ratio of 1:1:4. The recovered red gel was calcined at 700 °C for 3 h under argon flux. Two different samples were prepared by varying the aging time in triphenylantimony(III)–toluene–tertio-butanol solution, namely 48 h (sample SbC-1) and 24 h (sample SbC-2).

The morphology of the samples was investigated by scanning electron microscopy (SEM) analysis performed using a FEI Quanta 200 microscope coupled with EDX elemental analysis and by transmission electron microscopy (TEM) using a JEOL 1200 EX II microscope. The structure of the samples was controlled by XRD, using a D-max Ultima$^+$ Rigaku X-ray diffractometer.

The potentiodynamic cycling with galvanostatic acceleration (PCGA) was performed with a stepwise potential scans of 5 mV and a minimum current limits of 20 μA within a 0.01–2 V voltage limits using a VMP Biologic-Science Instruments in a three electrode cell where the Sb–C sample working electrode was combined with a lithium counter electrode and a lithium reference electrode. The Sb–C electrode was formed as a thin film by doctor-blade deposition on a copper substrate of a slurry composed of 80% Sb–C (active material), 10% PVdF 6020, Solvay Solef (binder) and 10% SP carbon (electronic support) for the sample. The electrolyte was a 1 M $LiPF_6$ solution in an ethylene carbonate–dimethyl carbonate, EC:DMC 1:1 (Merck Battery Grade) electrolyte soaked on a Whatman^{TM} separator.

The galvanostatic cycling of the Sb–C sample was performed in a two-electrode cell similar to the previous one with the exclusion of the reference lithium electrode, at a current density of 100 mA cm^{-2} g^{-1} within a 0.01–2 V voltage limit.

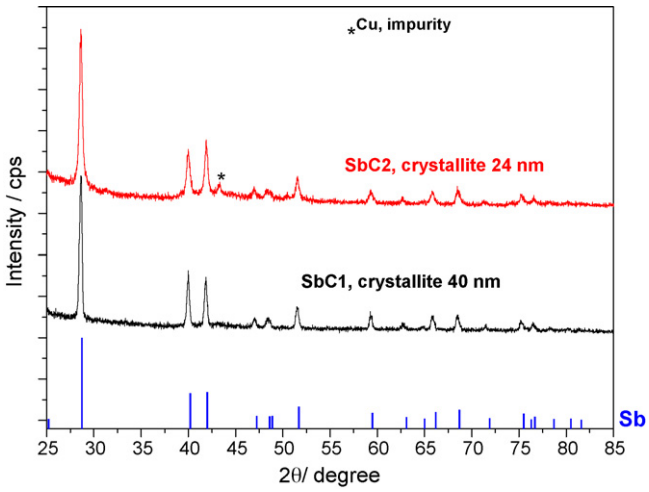

Fig. 1. XRD patterns of the samples SbC-1 and SbC-2.

3. Results and discussion

Two samples, here identified as SbC-1 and SbC-2, have been prepared as nanocomposites of antimony particles dispersed in a carbon matrix.

Fig. 1 shows the related XRD analysis. As expected, both patterns display the peaks of metallic antimony. However, the Rietveld refinement revealed that the samples differ by the average Sb crystallite size, being 40 nm for sample SbC-1 and 24 nm for sample SbC-2. The different synthesis conditions, which involved different period of contact of the gel with the solution containing the organometallic precursors (see Section 2) may account for this difference in crystallite size. It is reasonable to assume, in fact, that the time of immersion may influence the size of the Sb particles: a prolonged time, as in the case of sample SbC-1, can induce a higher swelling of the the gel structure with more consistently filling of Sb precursor into the material pores and thus, promoting the increase of the crystallite size during the final calcination step. Accordingly, the two samples also differ by the relative Sb content in the composite which, as determined by EDS elemental analysis, is 66 wt% for sample SbC-1 and 34 wt% for sample SbC-2.

The comparison of the two SEM images reported in Fig. 2 reveals the difference between the two samples in terms of surface morphology. Clearly, in the sample SbC-1 the Sb particles are distributed as large size aggregates, i.e. of the order of 500 nm, on the carbon

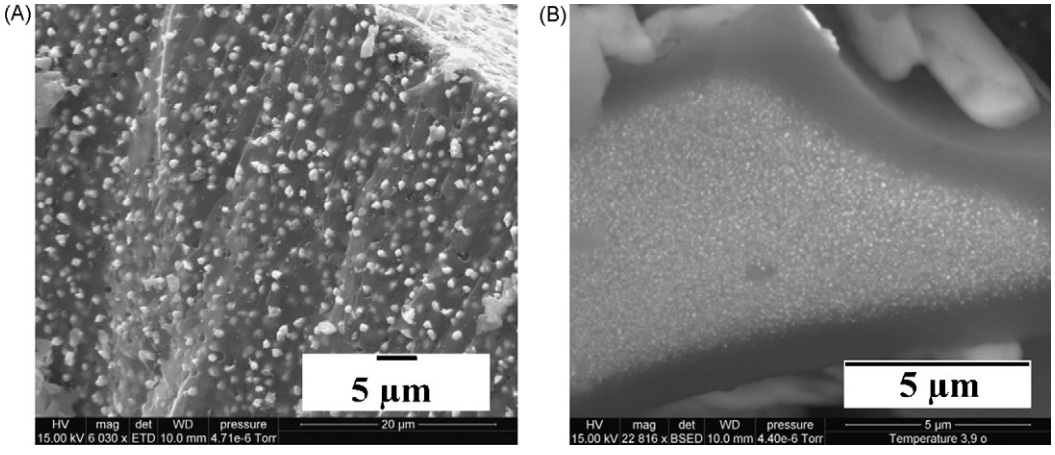

Fig. 2. SEM images of the samples SbC-1 (A) and of the sample SbC-2 (B).

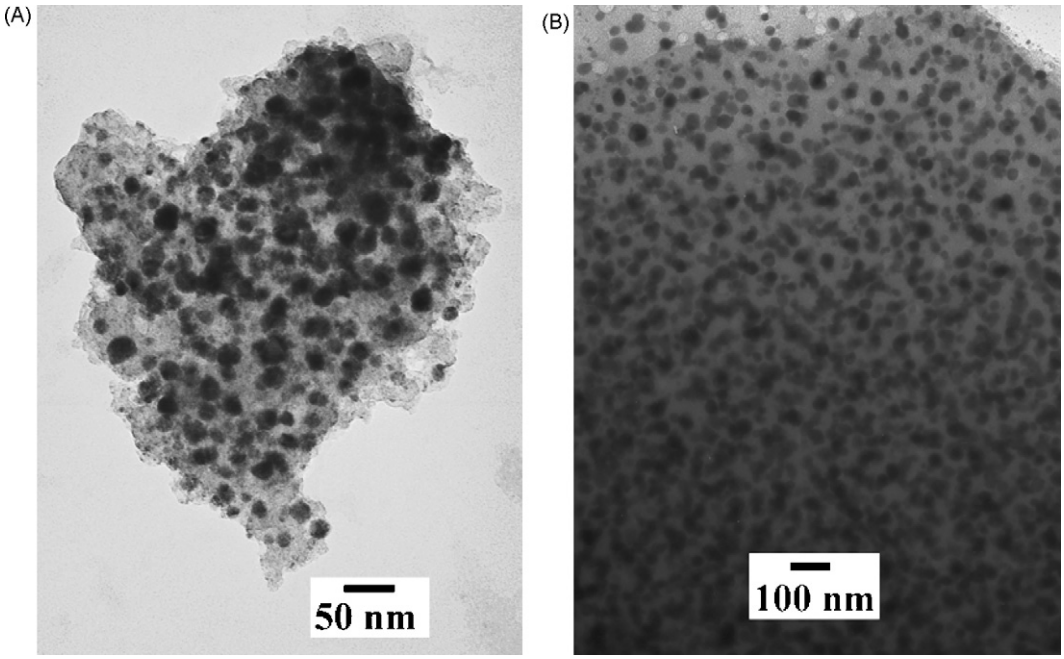

Fig. 3. TEM images of the samples SbC-1 (A) and of the sample SbC-2 (B).

matrix surface, while sample SbC-2 is characterized by smaller Sb particles, i.e. of the order of 50 nm, which are regularly distributed on the carbon matrix surface.

In contrast, the bulk morphology of the two samples is similar. From the TEM images reported in Fig. 3, it is possible to see in both cases a common regular distribution in the carbon matrix of Sb particles having an average size of 10–50 nm.

The difference of the particle size observed for sample SbC-1 when passing from the surface to the bulk can again be related to the synthesis conditions and in particular to the impregnation time of the gel by the solution of the antimony precursor. A high swelling time, as it is the case for SbC-1, favours the filling of the surface gel pores which are in average larger than those in the bulk, this in turn leading to the formation, during the final calcinations step, of the large surface particles. This surface agglomeration process is instead prevented in the case of sample SbC-2, where the short swelling time prevents the filling of the surface pores.

It is expected that this difference in size and distribution of the Sb particles may influence the electrochemical behaviour of the two samples. To verify this, we have prepared the two samples as film electrodes and tested them in cells using lithium metal as the counter electrode and a $LiPF_6$-EC-DMC solution as electrolyte. For both Sb–C samples, the expected main, reversible electrochemical process is the lithium alloying in antimony [15], which develops in two steps:

$$2Li + Sb \leftrightarrows Li_2Sb \quad (1)$$

$$Li + Li_2Sb \leftrightarrows Li_3Sb \quad (2)$$

with an associated total specific capacity of 660 mAh g^{-1}. In addition, also a side process of lithium intercalation in the carbon matrix:

$$xLi + yC \leftrightarrows Li_xC_y \quad (3)$$

cannot be excluded.

On the basis of the Sb:C composition, determined as 66 wt% and 34 wt% for sample SbC-1 and SbC-2, respectively and also on the basis of an analysis carried out in previous works dealing with similar metal–carbon composite [7], one may estimate the capacity associated to carbon as ca. 15 mAh g^{-1} and 30 mAh g^{-1}, respectively. Thus, the resulting overall capacity for the two samples is assumed to be ca. 450 mAh g^{-1} for SbC-1 and 255 mAh g^{-1} for SbC-2.

The electrochemical response of the two sample electrodes was first analyzed by PCGA (potentiodynamic cycling with galvanostatic acceleration), i.e., a powerful technique for the characterization of electrochemical processes [16]. Fig. 4A shows the PCGA profiles of the electrode sample SbC-1. Four reversible peaks, marked as 1–4, are clearly revealed; of these, peaks 1 and 4 are assumed to be representative of process (1) while peaks 2 and 3 of process (2), with an associated voltage in the region of 0.9 V vs. Li for the alloying process (1) and of 1.0 V vs. Li for the consequent de-alloying process (2). However, the figure also reveals at lower voltage regions the occurrence of irreversible processes, probably associated with structural rearrangements and/or to synthesis residual impurities in the carbon matrix.

Fig. 4B shows the PCGA of electrode samples SbC-2. The peaks representative of the main reversible process evolve in the same 0.9–1.0 V region but they are not as sharp as in the case of SbC-1, but rather merge in large peaks. This is not surprising due to the difference in particle morphology of the two samples: while SbC-1, having surface particles of the order of 500 nm, acts as a macrosize electrode with associated well defined PCGA voltage profiles, SbC-2 falls in the category of nanoelectrodes for which the voltage profiles tend to merge in an indistinguishable fashion [17]. To be also noticed that the low voltage irreversible peaks are larger than in the case of SbC-1. Considering that the amount of carbon doubles in SbC-2, the observed higher extension of the low voltage peaks seems to confirm their attribution to impurities present in the carbon matrix.

The differences in the electrochemical behaviour of the two electrodes are confirmed by their typical cycling responses in a lithium cell. Fig. 5A illustrates the voltage profiles of the SbC-1 sample. The first discharge shows a plateau in the region of 0.9–1.0 V, representing the main alloying process, however, with a total specific capacity largely exceeding than the theoretical value, this being associated

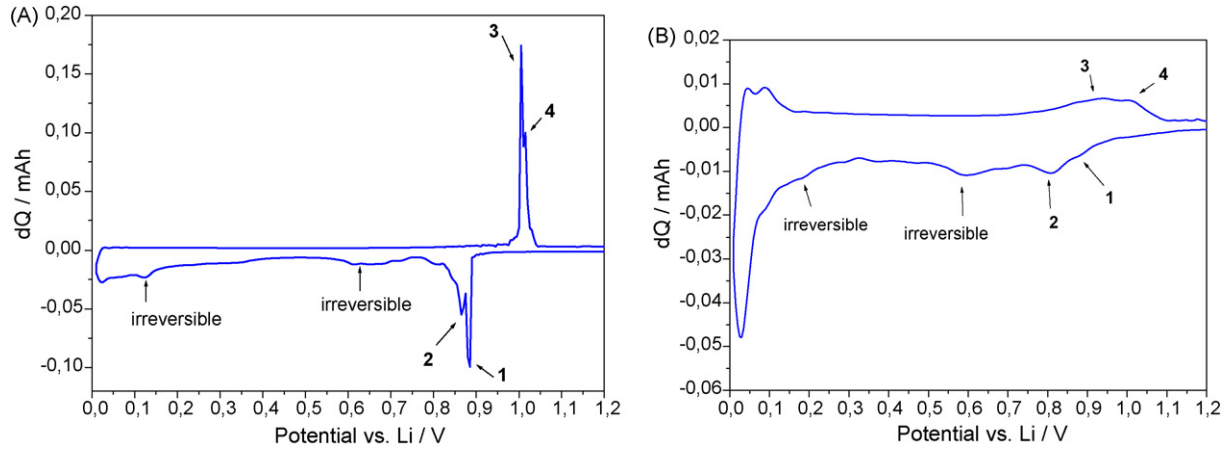

Fig. 4. Potentiodynamic cycling with galvanostatic acceleration (PCGA) of the samples SbC-1 (A) and SbC-2 (B). Stepwise potential scans: 5 mV; minimum current limits: 20 μA. Room temperature.

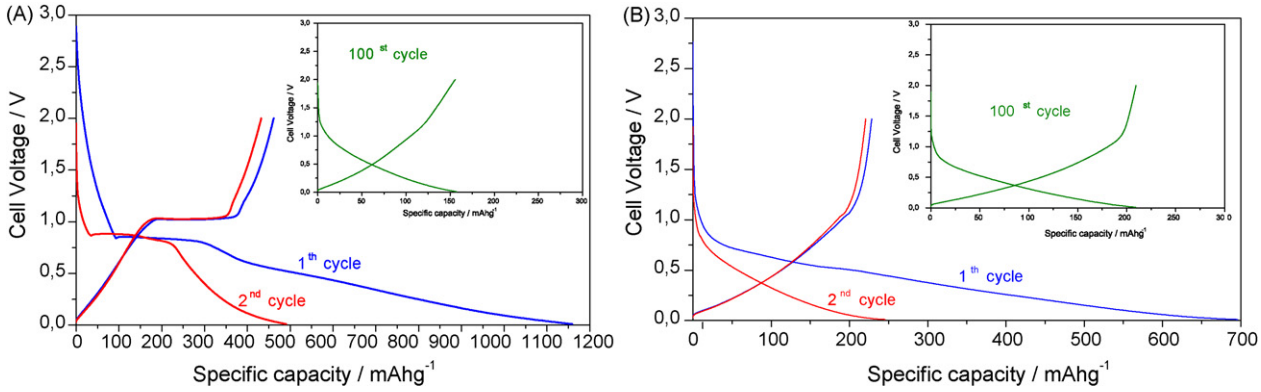

Fig. 5. Voltage vs. specific capacity of the lithium cells prepared using the sample SbC-1 (A) and SbC-2 (B). Electrolyte: $LiPF_6$ 1 M/EC:DMC 1:1; current density: 100 mA cm^{-2} g^{-1}; voltage limits: 0.01–2 V. Room temperature.

with the low voltage irreversible process (see Fig. 4 and related discussion). The following charge profile shows the plateau associated with the main reversible de-alloying process with a specific capacity of the order of 450 mAh g^{-1}. This value, which is that expected by the sample composition (see above), is reversibly reproduced in the following few charge–discharge cycles. To be noticed that, upon prolonged cycling, the voltage profile assumes a plateau-less, continuous behaviour with a consistent decay in specific capacity (see inset).

Fig. 5B shows the voltage profiles of the initial cycles of the SbC-2 electrode in the same type of lithium cell. In consistency with the PCGA response, this nanostructured electrode does not show net plateaus but rather continuous curves where the regions related to the main Sb alloying processes are not easily distinguishable. In this case, the larger amount of carbon reflects into a larger extent of the irreversible capacity, this leading to a reversible value limited to 250 mAh g^{-1}, which in fact is that expected on the basis of our calculation. To be noticed, however, that, contrary to the case of SbC-1, this value of capacity remains stable over prolonged cycling (see inset).

Fig. 6 shows the capacity delivery upon cycle number of the two electrodes tested in similar lithium cell. Electrode SbC-1 (Fig. 6A)

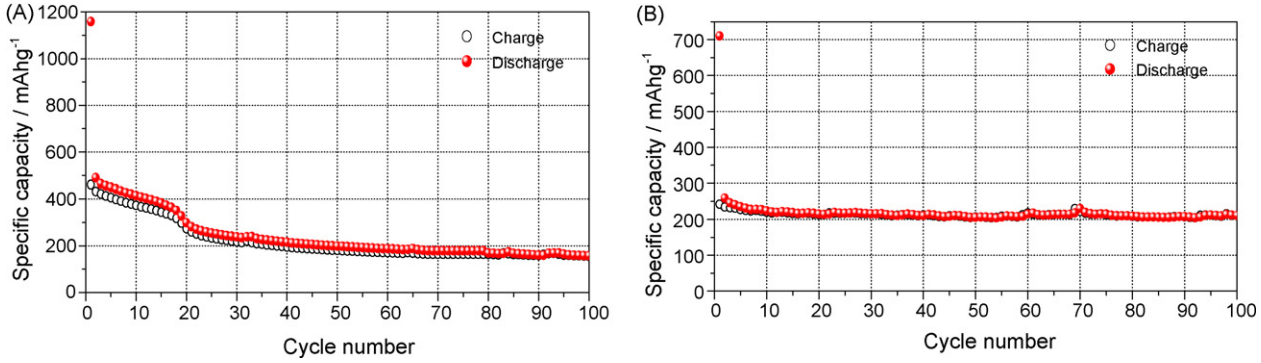

Fig. 6. Specific capacity vs. cycle number profile of the lithium cells prepared using the sample SbC-1 (A) and SbC-2 (B). Electrolyte: $LiPF_6$ 1 M/EC:DMC 1:1; current density: 100 mA cm^{-2} g^{-1}; voltage limits: 0.01–2 V. Room temperature.

delivers the expect full capacity, i.e. of the order of 450 mAh g^{-1}, only for few initial cycles, after which the capacity decays and remains at a lower value of ca. 200 mAh g^{-1} for the entire duration of the test (100 charge–discharge cycles). This behaviour is similar to that reported by other authors [8,12,14] and confirms the strict dependence of the electrode stability upon the particle size of the constituent material. It is then reasonable to assume that large particles cannot support the mechanical stresses associated to the large volume changes experienced during the alloying–de-alloying electrochemical process, this resulting in disintegration with associated loss of electronic contact between the active metal material and the current collector.

Different is the case of electrode SbC-2, see Fig. 6B. As expected by the lower Sb content, the initial capacity is lower than that of electrode SbC-1, i.e. 220 mAh g^{-1} versus 450 mAh g^{-1}. However, the capacity delivery remains stable with no appreciable decay over 100 charge–discharge cycles. To be noticed that the steady capacity of SbC-2 is similar in value to that assumed by SbC-1 after the initial decay, compare Fig. 6A. One may then be tempted to assume that in samples with a not uniform particle size distribution, the larger particles, as those on the surface of sample SbC-1 (see Fig. 3) rapidly disintegrate leading to the observed initial capacity decay, while the steady stable capacity delivery is assured by the remaining smaller particles placed in the core of the sample. This, however, is only a speculation and further investigation is needed to confirm the proposed particle model.

4. Conclusion

The results reported in this paper suggest that the poor cycling stability generally observed for the lithium–antimony alloy electrode, is probably due a lack of morphological optimization. In this respect, the role of the particle size appears to be crucial for sustaining the volume strains associated to the electrochemical process and thus for keeping a steady capacity delivery of the electrode. We show that even 500 nm is a too large size to assure the strain control and thus, a stable electrode performance. This condition may be achieved by reducing the particle size to a few nanometer level and by assuring an uniform particle distribution throughout the electrode mass. We show that under this configuration, Li–Sb electrodes can indeed operate with a stable capacity delivery. The value of capacity, however, is still too low to make these electrodes of direct practical interest. The challenge is to increase the amount of antimony in the carbon composite without undergoing particle aggregation so that to achieve an increase of the electrode capacity and its steady delivery on prolonged cycling. Work to achieve this goal is in progress in our laboratory.

Acknowledgements

This work has been carried out with the financial support of the Italian Ministry of University and Research under a PRIN 2005 project.

References

[1] J.M. Tarascon, M. Armand, Nature 414 (2001) 359.
[2] R.A. Huggins, in: G. Abbas Nazri, G. Pistoia (Eds.), Lithium Batteries, Kluwer Academic Publishers, Boston, 2004, p. 270.
[3] M. Winter, J.O. Besenhard, Electrochimica Acta 45 (1999) 31.
[4] J.R. Dahn, et al., in: G. Pistoia (Ed.), Lithium Batteries—New Materials, Developments and Perspectives, Elsevier, North Holland, 1993, pp. 1–47 (Chapter 1).
[5] M. Wachtler, M. Winter, J.O. Besenhard, J. Power Sources 105 (2002) 151.
[6] M. Winter, J.O. Besenhard, M.E. Spahr, P. Novak, Adv. Mater. 10 (1998) 725.
[7] G. Derrien, J. Hassoun, S. Panero, B. Scrosati, Adv. Mater. 19 (2007) 2336.
[8] R. Alcántara, F.J. Fernández-Madrigal, P. Lavela, J.L. Tirado, J.C. Jumas, J. Olivier-Fourcade, J. Mater. Chem. 9 (1999) 2517.
[9] F.J. Fernández Madrigal, P. Lavela, C. Pérez-Vicente, J.L. Tirado, J. Electroanal. Chem. 501 (2001) 205.
[10] X. He, W. Pu, L. Wang, J. Ren, C. Jiang, C. Wan, Electrochimica Acta 52 (2007) 3651.
[11] M. Morcrette, D. Larcher, J.M. Tarascon, K. Edström, J.T. Vaughey, M.M. Thackeray, Electrochimica Acta 52 (2007) 5339.
[12] A. Caballero, J. Morales, L. Sánchez, J. Power Sources 175 (2008) 553.
[13] A. Dailly, J. Ghanbaja, P. Willmann, D. Billaud, J. Power Sources 136 (2004) 281.
[14] C.M. Park, S. Yoon, S.I. Lee, J.H. Kim, J.H. Jung, H.J. Sohn, J. Electrochem. Soc. 154 (2007) A917.
[15] R.A. Huggins, J. Power Sources 26 (1989) 109.
[16] A.H. Thompson, J. Electrochem. Soc. 126 (1979) 608.
[17] L.F. Nazar, G. Goward, F. Leroux, M. Duncan, H. Hung, T. Kerr, J. Gaubicher, Int. J. Inorg. Chem. 3 (2001) 191.